



# Hydrochemistry and isotope hydrology of groundwater and surface water in the Sor and Gebba watershed, southwestern Ethiopia

Wondmyibza Tsegaye Bayou<sup>1,3</sup> · Mebruk Mohammed<sup>1</sup> · Tenalem Ayenew<sup>2</sup> · Tesfay Kiros Mebrahtu<sup>3</sup> · Stefan Wohnlich<sup>3</sup>

Received: 3 August 2023 / Accepted: 27 April 2024  
© The Author(s) 2024

## Abstract

The Sor and Gebba watershed plays a crucial role in the water resources of the Baro-Akobo River Basin. However, various factors have had a detrimental effect on the watershed. Unplanned groundwater extraction, wetland drainage, surface water pollution, and land use changes have all intensified due to population growth, urbanization, commercial farms, industrial development, poor water resources management, and improvements in living standards. This research utilized major hydrochemical ions and environmentally stable isotopes to elucidate the interaction between groundwater and surface water in the watershed, which are reliable tracers in various hydrologic processes. During the 2020 wet season and 2022 dry season, over 25 meteoric water samples were collected from different locations for hydrochemical and isotopic analysis. The hydrochemical analysis revealed that the dominant water type is Ca–Mg–HCO<sub>3</sub><sup>−</sup>. Among the anions, HCO<sub>3</sub><sup>−</sup> was the most dominant, followed by NO<sub>3</sub><sup>−</sup>, Cl<sup>−</sup>, and SO<sub>4</sub><sup>2−</sup>, and those of cations Ca<sup>2+</sup>, followed by Na<sup>+</sup>, Mg<sup>2+</sup>, and K<sup>+</sup>. The spatial analysis of environmentally stable isotopes confirmed the interaction between groundwater and surface water in the watershed. The quality of groundwater is primarily influenced by rock-water interaction (Gibb's diagram) and, to some extent, by evaporation (Isotope study). A graph of the water samples closely aligned with the Addis Ababa-local meteoric water line indicates their meteoric origin. However, there was a slight deviation to the left due to the effects of distance and altitude. The isotopic correlation further supported the interaction between different water sources.

**Keywords** Groundwater · Isotope ratio · Major ions · Stable isotopes · Ethiopia

## Introduction

Mail: wond.tsege@gmail.com

Of all the resources necessary for living, water is essential to sustain all kinds of life on Earth. Although water is plentiful, it is frequently scarce and characterized by an uneven spatiotemporal distribution (Melesse 2011; Brooks et al. 2013; Wang et al. 2019). In recent years, water demand

has generally increased rapidly with population growth, urbanization, industrial development, irrigated agriculture, improvements in living standards, and poor water resources management (Krishnaraj et al. 2012; Mengistu et al. 2021; Zhang et al. 2021).

Ethiopia has abundant naturally available water resources even though its distribution and occurrences are erratic in space and time (Chernet 1993; Berhanu et al. 2014; Mengistu et al. 2021). Groundwater (springs, shallow wells, and deep wells) is the most strategic and renewable natural resource, contributing over 90% of the domestic water supply for the rural and urban Ethiopian population in all climatic regions (Kebede 2013; Abteu and Dessu 2019; Mengistu et al. 2021).

People consider groundwater, surface water, and rainwater as separate water sources. However, all meteoric natural waters are from a single source and are components of the dynamic hydrologic cycle. Depletion or contamination of one of these sources could cause diminishment and

✉ Wondmyibza Tsegaye Bayou  
wondmyibza.bayou@rub.de; wond.tsege@gmail.com

<sup>1</sup> School of Civil and Environmental Engineering, Addis Ababa Institute of Technology, Addis Ababa University, PO Box 385, Addis Ababa, Ethiopia

<sup>2</sup> College of Natural Science, School of Earth Sciences, Addis Ababa University, PO Box 1176, Addis Ababa, Ethiopia

<sup>3</sup> Institute of Geology, Mineralogy and Geophysics, Ruhr Universität Bochum, Universitätsstra. 150, 44801 Bochum, Germany

deterioration of others by changing their quantity and quality since groundwater and the other sources are interdependent and interconnected with each other in many ecosystems (Fetter 2001; Dingman 2015; Ezugwu and Apeh 2017). The quantity of one of these sources can also affect the other in terms of flow, hydrochemistry, and temperature. The construction of dams and other hydraulic structures could also alter the situation.

Only after 1925 was the existence of oxygen isotopes observed by Giaque and Johnston (Grauque and Johnston 1929; Garrett 1962). This preceding work led Urey to an initial theoretical study investigating Deuterium (D) within the naturally occurring meteoric water (Urey 1931; Rundel et al. 1989). Then several researchers (Fritz et al. 1979; Stuyfzand 1989; Devito et al. 1996; Leontiadis and Nikolaou 1999; Reimer et al. 2009) recommended the assessment of environmental stable isotopes (ESI) of D and Oxygen-18 and major hydrochemical ions (MHI). Recent advances in isotope ratio mass spectrometry (IRMS) enabled the measurement of the ratio of stable isotopes (Abid et al. 2011; King et al. 2014; Zhang et al. 2021) made a significant contribution to the research and study of groundwater-surface water (GW–SW) interaction and developments based on the hydrochemical ions and isotope analysis.

The Sor and Gebba watershed is the headwater of the Baro River that drains the Baro-Akobo River Basin from Ethiopia and joins the White Nile in South Sudan at Malakal. The watershed comprised many wetlands and streams distributed spatially throughout. Recently, the watershed faced considerable water resources problems and aquifer depletion due to, among others, groundwater over-abstraction, wetland drainage, surface water pollution, land use changes, and changes in hydrodynamics. Understanding the effect and the counter effect of these water resources stressors on the groundwater hydrology of this watershed is thus becoming important. MHI and ESI are relatively cheaper and yield plentiful information about the hydrologic cycle (Terwey 1984; Zhou et al. 2017; Barbieri 2019). The aim of this study is to (a) assess the spatial distribution of water types, (b) characterize hydrogeological conditions, and (c) explore the GW–SW interaction of meteoric natural waters.

## Description of the study area

The Sor and Gebba watershed is found in the Southwest part of the country. Geographically located between 35° 17' and 36° 18' east longitude and 7° 36'–8° 40' north latitude, it is 6556 km<sup>2</sup> of land in Oromia and the newly established South West Ethiopia Peoples' Region (SWEPR); furthermore, the details were mentioned by Bayou et al. (2021). As shown

in Fig. 1, the watershed covers wholly or partially seven districts (Weredas) of the Illubabor zone and three Weredas of the Jimma zone from the Oromia region, likewise three Weredas from the Keffa zone of the SWEPR.

Ethiopian climate is mainly controlled by the complex topography and the seasonal migration of the inter-tropical convergent zone (ITCZ) and is commonly defined together with temperature (Billi 2015). The cool to cold, elevated areas between 2300 and 3300 m above sea level (m.a.s.l.) are classified as Highland (Dega) with the mean annual temperature between 10 and 15 °C; the warm to cool, mildly elevated areas between 1500 and 2300 m.a.s.l. are grouped as Temperate (Woynadega) with the mean annual temperature between 15 and 20 °C; the warm to hot, elevated areas between 500 and 1500 m.a.s.l. are distinguished as Lowland (Kola) with the mean annual temperature of about 30 °C (Chernet 1993; Alemayehu 2006; Berhanu et al. 2014). The Sor and Gebba watershed temperature varies from 10 to 20 °C, and the altitude ranges from 963 to 2969 m.a.s.l. and is classified primarily under the Woynadega climatic region.

The watershed climate and forest cover are associated with the amount of precipitation. Similar to temperature and rainfall, evapotranspiration varies with elevation and location. The high evapotranspiration values known in the lowlands exceeded 1500 mm/year, whereas the low values in the highlands are nearly 1000 mm/year. According to the Ministry of Water and Energy (MoWE)-Ethiopian Meteorology Institute (EMI), this most humid southwest region receives over six months of rainfall yearly, with mean annual rainfall exceeding 1800 mm in several places, the highest being near Gore town, estimated at around 2400 mm/year (Bayou et al. 2021). The heavy summer (Keremt) rain occurs when the ITCZ is in the north. During this time, Equatorial Westerlies from the South Atlantic Ocean and winds blowing to the south from the Indian Ocean influence the whole country (Alemayehu 2006; Melesse 2011; Berhanu et al. 2014; Girmay et al. 2015). In this tropical watershed, precipitation decreases northwards with a decrease in altitude ranging from 1500 to 2200 mm/year.

This humid southwestern region has created favorable conditions for wetland and irrigated agriculture due to sufficient moisture year-round. The watershed rural community harvest depends mainly on cash crops and spices. Continuous production of these different types of Agro-industrial input crops could be possible through irrigation practices. Dense mixed high forests dominate the land use and land cover of the Sor and Gebba watershed. These forests and perennial crop cultivation cover over 70% of the land units in the watershed. Wooded grassland predominantly covers the low-lying areas of the watershed. Vegetation cover can be necessary for flood mitigation and GW–SW interactions.

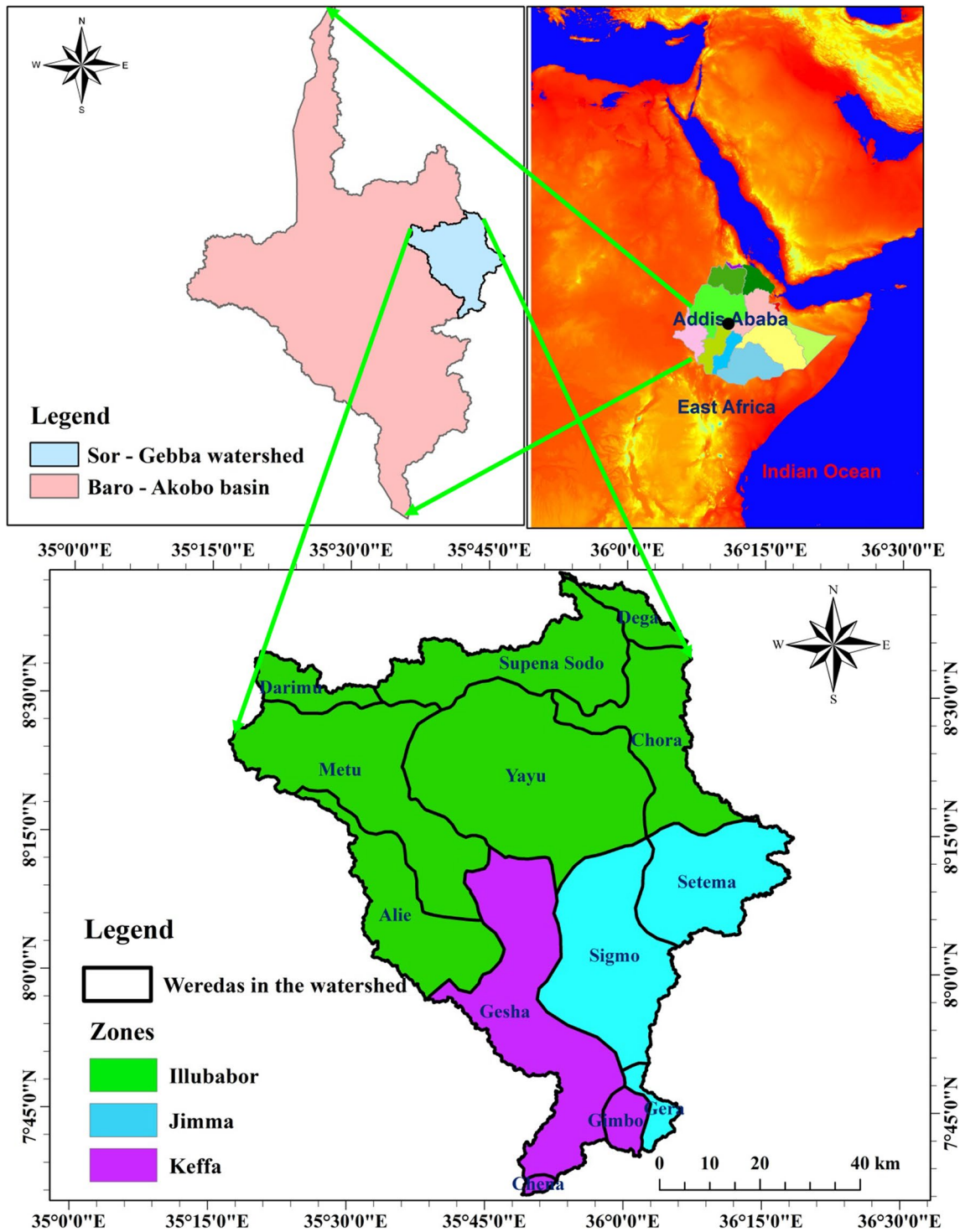


Fig. 1 Location map of the study area

### Geological and hydrogeological setting

The stratigraphic settings and associated tectonic phenomena significantly controlled the study area (Kazmin and Warden 1975; Chernet 1993; Bayou et al. 2021). Geologically, the

watershed is underlain by impermeable metamorphic Precambrian crystalline basement rocks (PCBR) and overlain with Tertiary to Quaternary volcanic rocks (QVR). Mostly weathered and fractured Tertiary volcanic rocks (TVR) are forming moderate aquifers. The remaining QVR cover

creates a poor aquifer, except in localities where it exhibits scoracious (Alemayehu et al. 2018). From the hydrogeological viewpoint, the uppermost part of the jointed, weathered, and fractured gneiss and TVR is considered the source of recharge for groundwater. However, the PCBR and QVR in the upper plateau are intact and massive. Geological structures created due to fracturing and tectonics might allow water transmission. However, marsh develops where rocks become impermeable near the surface (Chernet 1993; Bayou et al. 2021).

Geological and tectonic settings play a significant role in the process of groundwater discharge and recharge mechanism of watersheds. Springs are the most available sources of domestic water supply in topographically elevated headwater regions. These sources are inadequate during winter. Most springs emerging from volcanic rock are geology, topography, and structures controlled and are prone to change due to natural and anthropogenic activities. The regional geological formation includes Sillimante garnet gneiss that occurs along the Gebba stream north of Metu, gneissic-granite rocks of the Mozambique tectonic belt, such as the PCBR, Tertiary lower tracheae, Tertiary basalt flows, phonolites and tracheae dikes, and Quaternary alluvial loose sediments (Tefera et al. 1999; Bayou et al. 2021).

The watershed formations are gray biotite and hornblende gneisses, granulite, granodiorite, and migmatite with minor meta-sedimentary gneisses included under *the Alghe Group, also called the Alghe Gneiss (ARI)*; Pre to Syn-orogenic intrusive masses of granites, biotite, muscovite, named as orthogenesis or *Pre-tectonic to Syn-tectonic granitoid (Gtl)*; trachybasalts, rhyolites, felsic rocks, and flood basalts directly overlying the PCBR known as *the Jimma Volcanics (Pjb)*; *the Mekonnen basalts (PNmb)*; and ignimbrites, unwelded tuffs, ash flows, rhyolitic flows, domes, and trachyte units are known to be *the Nazret Series (Nn)* (Tefera et al. 1999; Bayou et al. 2021), and shown in Fig. 2. The soil derived from parent rocks of the PCBR and TVR created the main laterite soil, resulting in the watershed having less infiltration capacity. According to the FAO document (FAO 1984), the Sor and Gebba watershed is covered by Acrisols, Cambisols, and Lithosols. The larger watershed area is also influenced by soil acidity (Beyene et al. 2023).

### Hydrochemical ions and stable isotopes

Hydrochemical ions and stable isotopes are tools for insight into complex hydrogeological processes like sources, ages, directions of groundwater flow and interaction with surface water, and the impact of climate change on water resources development and management (Kendall and McDonnell 1998; Ragheb 2008; Zhang et al. 2021). Hydrogen and oxygen isotopes are commendable and proven water tracers because they constitute the water molecule and help identify

sources and amounts of recharge and estimate groundwater flow rates (Hunt et al. 2005; Anderson et al. 2015). The primary advantage of these isotopes is the natural provision of the input function or 'tracer injection' to the hydrological system.

Major hydrochemical ions ( $\text{Na}^+$ ,  $\text{K}^+$ ,  $\text{Ca}^{2+}$ ,  $\text{Mg}^{2+}$ ,  $\text{Cl}^-$ ,  $\text{HCO}_3^-$ ,  $\text{NO}_3^-$ , and  $\text{SO}_4^{2-}$ ) and natural ESI ( $\delta\text{D}$  and  $\delta^{18}\text{O}$ ) data analysis has been widely applied in the past decades for GW–SW interaction, in calibrating and validating numerical models, to determine hydrogeological conditions such as origin, flow pathways, sources of recharge, and other hydrochemical processes involving aquifers (Fritz et al. 1979; Clark 2015; Zhou et al. 2017). Isotopes in water, solutes, and solids tell us about the quality of groundwater, the evolution of geochemical processes, the processes regarding recharge, the rock and water interaction, and the source of contaminants (Clark 2015; Xiao Yu et al. 2022). Though their natural abundance is limited, isotopes involved in groundwater investigations are the heavy stable isotopes of a water molecule, D and  $^{18}\text{O}$ , and radioactive tritium isotopes (Terwey 1984). As air masses move across continents and lose water by a rainout, they become depleted in the heavy environmental isotopic species ( $\text{H}_2^{18}\text{O}$  and  $\text{HD}^{16}\text{O}$ ) because of the enrichment of the liquid phase with weighed isotopic species relative to the vapor phase (Kendall and McDonnell 1998; Tarbuck and Lutgens 2017).

The combined effect of different tracers ensures that the specific limitations of single tracers or methods could not bias our understanding of the hydrological system. Furthermore, the ESI method should also be combined and integrated with other hydrological and scientific approaches like hydrochemistry, hydrometry, geophysics, and remote sensing (Kendall and McDonnell 1998). These tracer techniques have the potential advantages of distinguishing and providing joint information, and they can be very efficient in characterizing complex systems in remote areas like the Sor and Gebba watershed.

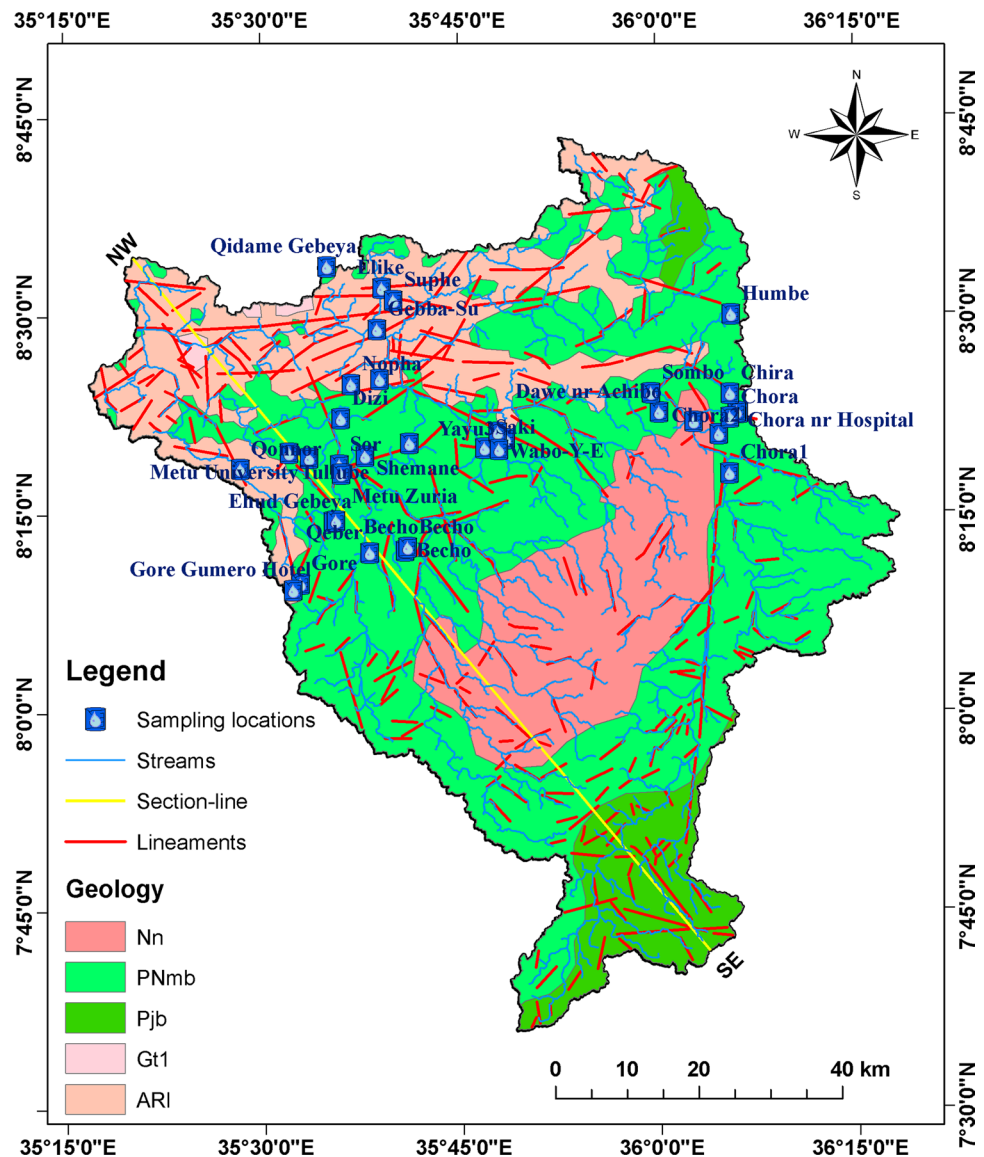
## Materials and methods

### Sample collection and testing

This section provides detailed materials and methods and subsequent analyses of field studies conducted during the Keremt 2020 and the Bega 2022. Representative water samples were collected from different meteoric water sources to assess the water types and interactions between streams and groundwater sources. Generally, protected water sources (streams, major springs, boreholes, deep wells, and wetlands) were selected where topography and hydrogeology allowed their replenishment areas to be well delineated and discerned.



**Fig. 2** Geological map (modified from GSE, 2005; 1: 250,000 scale), and areal distributions of samples (section in Fig. 8)



Over 25 water samples were repeated in triplicate from each location (two wetlands, nine wells, 11 springs, six streams, and rain) as collected from the field campaign for major hydrochemical ions and stable isotope analysis. Sampling for ions comprised two 50 mL bottles with screw caps; one graduated cylindrical plastic for anions sampling. These bottles were pretreated with blank water and rinsed using sampled water. The other polypropylene graduated conical centrifuge tubes were each treated with two drops of nitric acid (63% HNO<sub>3</sub>) and filtered with 0.45 μm membrane filters (Lot No. 20170112) for cations sampling. In most cases, samples are conserved by adding acid until the pH is below 2 (0.7 mL of 65% HNO<sub>3</sub> is usually sufficient to acidify a 100 mL sample). Acidification can stop the growth of most bacteria, inhibit oxidation reactions, and prevent the adsorption or precipitation of cations (Clark and Fritz 1997; Appelo and Postma 2005; Vreča and Kern 2020).

In-situ testing involves measuring electrical conductivity (EC), pH, and temperature by using portable digital multi-parameter water analyzers (HANNA-HI 8733 and HI 83141) and bicarbonate (HCO<sub>3</sub><sup>-</sup>) test by titration using sulfuric acid (H<sub>2</sub>SO<sub>4</sub>) and Bromo-cresol green-methyl red indicator. Major hydrochemical ions were measured using ion chromatography (IC). Sampling for isotope analysis involves filtering the sample using a 0.2 μm membrane filter (Lot No. 90287103) into 2 mL transparent high-performance liquid chromatography (HPLC) glass vials collected from Ruhr University Bochum (RUB) laboratories. Samples were collected carefully to avoid contamination during sampling and kept in respective bottles by tightly capping the lid.

The laboratory analysis involved measuring major cations (Na<sup>+</sup>, K<sup>+</sup>, Ca<sup>2+</sup>, and Mg<sup>2+</sup>) and anions (Cl<sup>-</sup>, NO<sub>3</sub><sup>-</sup>, and SO<sub>4</sub><sup>2-</sup>) using an IC (940 Professional IC Vario) and stable

isotopes of water (Deuterium and Oxygen-18) using an isotope ratio mass spectrometer (IRMS). The laboratory analysis was carried out in the Hydrogeochemistry laboratory and Sediment and Isotope Geology laboratory in the RUB in Germany. The analytical procedures and results were of scientific standards. Besides, the recent field sampling incorporated data

of the isotopic abundance ratio of a sample with the standard (VSMOW) designated by a delta ( $\delta$ )-value, given in per mille (‰). Stable isotope concentrations are measured as a ratio of the rare to the abundant isotope and expressed as the difference in this ratio between the sample and a known reference (Eq. 3):

$$\delta^{18}\text{O}_{\text{sample}} = \left( \frac{(\text{18O/16O})_{\text{sample}} - (\text{18O/16O})_{\text{reference}}}{(\text{18O/16O})_{\text{reference}}} \right) * 1000 \text{permilVSMOW} \quad (3)$$

from previous water quality studies to enhance the research quality.

### Major ions and isotopes

This research, examining groundwater and surface water using major ions, was supported by data collected from the local water resources office. The ion balance error (IBE) estimates the analysis accuracy for major ions since the sum of positive and negative charges in the water sample should be equal (Eq. 1). Differences in charge balance of up to 2% are inevitable in almost all laboratories, but with deviations above 5%, sampling and analytical procedures should be examined. Cations and anions were expressed in meq/L and inserted without their charge sign (Freeze and Cherry 1979; Appelo and Postma 2005; Clark 2015).

$$\text{Ion balance} : \sum \text{Cations} = \sum \text{Anions} \quad (1)$$

However, the analytical errors cause an ion imbalance called the IBE and it is calculated from (Eq. 2).

$$\text{IBE}(\%) = \left( \frac{\sum \text{Cations} - \sum \text{Anions}}{\sum \text{Cations} + \sum \text{Anions}} \right) * 100 \quad (2)$$

An IBE exceeding  $\pm 5\%$  should result in the analysis being rejected and excluded from interpretation. In this study, all the sampling data analysis results in IBE (Tables 1, 2, 3) of the acceptable limit range from  $-1.96$  to  $2.96$  for primary data and from  $-4.94$  to  $4.31$  for secondary data obtained from Metu water resources office ensuring its reliability. Therefore, an attempt was made to include the results of these secondary sources for further interpretative analysis.

Deuterium and Oxygen-18 are tracers of water movement and are used to study groundwater-surface water interactions, sources, and contaminants in water. Currently, groundwater processes, geochemical reactions, and complex water processes are detected using ESI (Clark 2015; Kebede and Zewdu 2019; Zhang et al. 2021). The divergence

where: delta ( $\delta$ ) indicates the difference in ratio from the standard, VSMOW (Vienna Standard Mean Ocean Water) is the standard, ‰ is the per mille notation.

Since most natural waters contain fewer 'heavy' isotopes than the standard, the  $\delta$ -values of samples in most cases remain negative.

### The procedure of isotope data analysis

Both hydrogen and oxygen isotope data are integral parts of the natural meteoric water molecules. In determining deuterium and oxygen-18 from a given water source, a 2 mL sample was collected from each sampling location. After sample preparation and transfer into a sample gas, isotopic abundance analysis was conducted by IRMS.

Water samples were collected in 1.5 mL vials without headspace closed with screw caps with a septum and stored in a refrigerator at 5 °C until analysis. During analysis, the samples were placed in an auto-sampler Thermo-Fisher Scientific (TFS-AS 3000), and the analysis of hydrogen and oxygen isotope values was conducted with a Continuous-Flow-Isotope-Ratio-Mass-Spectrometer (CF-IRMS) 253 plus (TFS) equipped with a ConFloIV and a TC/EA (High-Temperature Conversion Elemental Analyzer; both TFS). The syringe size was 10  $\mu\text{L}$ , and a sample volume of 1.5  $\mu\text{L}$  was injected into the TC/EA.

Before and after sample injection, the syringe was rinsed with blank water, and before sample injection, the syringe was rinsed three times with the sample water in addition to three plunger strokes before sample uptake for injection. The Pre-Injection dwell-time was two seconds, and the Post-Injection dwell-time was one second. The injected sample was transferred into the TC/EA reactor filled with glassy carbon granulate at a temperature of 1400 °C. Heating allows converting  $\text{H}_2\text{O}$  into  $\text{H}_2$  and  $\text{CO}$  gas. The TC/EA Gas Chromatography-Column Temperature was set to 90 °C. Data were presented as delta

**Table 1** Results of water samples analysis collected for the Keremt of 2020 sampling

S. no.	Location name	Source (origin)	Lon X (E) (UTM)	Lat Y (N) (UTM)	Elevation (m.a.s.l.)	Date collected	Temp. (°C)	pH	EC (µS/cm)	Cations (mg/L)			Anions (mg/L)			Ion balance error (%)		
										Ca <sup>2+</sup>	Mg <sup>2+</sup>	Na <sup>+</sup>	K <sup>+</sup>	NO <sub>3</sub> -N	HCO <sub>3</sub> <sup>-</sup>		Cl <sup>-</sup>	SO <sub>4</sub> <sup>2-</sup>
<i>I. Primary data collected from field in 2020</i>																		
1	Sor (Metu)	SRI	0786141	0919692	1519	26.9.2020	30.5	6.95	353	3.95	1.44	1.29	0.73	1.50	19.00	0.70	0.70	2.71
2	Saki (Yayu)	SRI	0806355	0922062	1308	26.9.2020	22.0	7.65	510	10.25	3.75	4.25	0.94	2.60	47.00	1.40	6.40	2.16
3	Qonnor (Burusu)	SRI	0772335	0919052	1571	27.9.2020	26.8	7.00	373	4.32	1.50	1.30	0.35	0.50	21.00	0.80	0.60	2.12
4	Qeber (Kemise)	SRI	0790393	0907402	1674	28.9.2020	21.5	5.42	336	5.38	1.74	1.71	0.46	0.20	28.00	0.60	0.50	0.87
5	Elike (Suphe)	SRI	0792056	0944371	1570	29.9.2020	27.4	6.23	308	4.27	1.41	1.60	0.46	1.10	22.00	0.40	0.40	1.57
6	Gebba (Suphe)	SRI	0791389	0938602	1136	29.9.2020	23.7	7.23	325	6.60	2.13	2.01	1.14	1.70	31.00	0.90	1.20	2.96
7	Shemane (Metu)	GWS	0789745	0920922	1669	26.9.2020	21.8	5.50	350	3.65	1.09	0.94	0.10	4.90	12.00	0.70	0.60	1.62
8	Wobo (Yayu-Metu)	GWS	0809328	0923353	1550	26.9.2020	34.0	7.23	1565	18.82	6.43	6.75	2.20	9.00	100.0	0.90	0.30	0.07
9	Wabo (Yayu-Elemo)	GWS	0808247	0924237	1561	26.9.2020	22.1	5.34	875	6.98	1.91	7.43	1.34	13.20	33.00	1.60	1.20	2.31
10	Becho	GWS	0795311	0907730	1752	28.9.2020	20.8	4.70	553	3.07	0.79	0.21	0.32	5.10	8.00	0.80	0.10	-0.53
11	Qidame Gebeya	GWS	0784391	0947363	1712	29.9.2020	26.4	4.92	850	8.06	2.70	3.03	0.10	28.80	14.00	2.30	0.10	-0.16
12	Suphe	GWS	0793672	0942664	1654	29.9.2020	23.4	5.95	1160	14.18	5.82	8.02	2.35	4.80	95.00	0.40	0.10	-1.61
13	Nopha	GWS	0787763	0930935	1701	29.9.2020	25.0	5.06	3310	16.31	7.24	13.30	7.75	76.80	10.00	24.8	1.60	1.18
14	Ehud Gebeya	GWS	0785289	0911739	1683	30.9.2020	21.3	5.17	986	11.24	3.07	3.92	0.70	22.30	32.00	3.70	0.50	0.16
15	Gore	GWS	0780750	0903090	1986	30.9.2020	18.1	5.75	733	8.17	1.64	4.91	2.29	13.90	25.00	5.30	0.80	0.90
16	Yember nr Chora	GWS	0839058	0924097	1890	1.10.2020	20.6	5.13	940	11.68	3.14	3.72	1.25	17.50	38.00	4.20	0.50	0.08
17	Dawe nr Achibo	GWS	0830706	0927100	1576	1.10.2020	21.3	6.34	2830	21.71	10.97	21.8	3.17	4.60	164.0	1.30	2.20	2.88
18	Becho	GWS	0795666	0908167	1781	28.9.2020	18.0	5.82	230	2.37	0.12	0.10	0.49	3.10	5.00	0.20	0.20	1.20
19	Tullube	GWD	0779128	0921347	1670	27.9.2020	26.4	5.30	575	3.97	1.24	2.50	1.52	13.90	10.00	1.30	0.10	2.36
20	Becho	GWD	0795666	0908167	1781	28.9.2020	19.9	4.62	2060	21.40	7.06	18.7	4.41	22.90	120.0	6.30	0.10	1.15
21	Metu nr University	GWD	0781956	0920603	1654	30.9.2020	25.0	4.70	790	8.71	2.01	3.52	0.36	28.40	12.00	3.40	0.30	0.37

Table 1 (continued)

S. no.	Location name	Source (origin)	Lon X (E) (UTM)	Lat Y (N) (UTM)	Elevation (m.a.s.l.)	Date collected	Temp. (°C)	pH	EC (µS/cm)	Cations (mg/L)			Anions (mg/L)			Ion balance error (%)		
										Ca <sup>2+</sup>	Mg <sup>2+</sup>	Na <sup>+</sup>	K <sup>+</sup>	NO <sub>3</sub> -N	HCO <sub>3</sub> <sup>-</sup>		Cl <sup>-</sup>	SO <sub>4</sub> <sup>2-</sup>
22	Ehud Gebeya Mosque	GWD	0785655	0911900	1738	30.9.2020	20.6	5.67	2480	11.50	3.46	6.21	36.8	21.00	56.00	8.20	22.4	2.87
23	Gore Gumero Hotel	GWD	0779707	0902211	2003	30.9.2020	19.8	4.02	2120	11.47	3.07	12.87	14.1	59.80	10.00	19.6	1.50	0.90
24	Chora inside Hospital	GWD	0841808	0927057	1990	1.10.2020	20.9	5.00	373	5.15	0.69	1.17	4.94	1.60	23.00	0.80	1.90	2.77
25	Abono nr Chora	GWD	0835534	0925790	1633	1.10.2020	20.7	5.80	1638	20.92	5.73	7.60	1.38	2.50	105.0	0.70	1.10	2.11
26	Hurumu town	GWB	0795938	0922714	1783	26.9.2020	27.9	7.35	3460	31.90	18.38	15.0	4.34	0.20	240.0	0.70	0.70	-1.33
27	Chora nr Hospital	GWB	0841515	0927141	1962	1.10.2020	23.0	5.85	1296	7.41	1.25	1.37	2.24	3.20	30.00	2.00	0.10	-1.02
						Max	34.0	7.65	3460	31.90	18.38	21.8	36.8	76.8	240.0	24.8	22.4	2.96
						Min	18.0	4.02	230	2.37	0.12	0.10	0.10	0.20	5.00	0.20	0.10	-1.61
						Avg	23.3	5.77	1162.2	10.50	3.70	5.75	3.56	13.52	48.52	3.48	1.71	1.14



**Table 2** Results of water samples analysis collected for the Bega of 2022 sampling

S. no.	Location name	Source (origin)	Lon X (E) (UTM)	Lat Y (N) (UTM)	Elevation (m.a.s.l.)	Date collected	Temp. (°C)	pH	EC (µS/cm)	Cations (mg/L)			Anions (mg/L)			Ion balance error (%)		
										Ca <sup>2+</sup>	Mg <sup>2+</sup>	Na <sup>+</sup> K <sup>+</sup>	NO <sub>3</sub> -N	HCO <sub>3</sub> <sup>-</sup>	Cl <sup>-</sup>		SO <sub>4</sub> <sup>2-</sup>	
<i>2. Primary data collected from field in 2022</i>																		
1	Saki (Yayu)	SRI	0806355	0922062	1308	1.3.2022	23.3	7.05	545	23.1	4.9	9.0	4.2	5.69	100	3.34	3.70	-0.33
2	Qonnor (Bursa)	SRI	0772335	0919052	1571	26.2.2022	19.0	6.46	466	20.8	3.0	7.3	4.5	2.49	95	1.35	0.90	0.83
3	Qeber (Kemise)	SRI	0790393	0907402	1674	23.2.2022	23.0	6.84	392	20.6	3.9	6.9	28.4	17.60	120	1.74	0.86	0.49
4	Elike (Suphe)	SRI	0792056	0944371	1570	2.3.2022	21.1	7.29	345	17.7	3.1	7.3	7.7	46.20	45	3.29	1.09	0.25
5	Gebba (Suphe)	SRI	0791389	0938602	1136	2.3.2022	22.6	7.35	447	13.1	3.2	5.9	7.1	57.72	12	2.18	2.16	0.69
6	Gebba (Chora)	SRI	0833214	0926994	1540	24.2.2022	22.0	4.80	275	7.7	2.2	4.9	8.2	9.77	42	1.52	1.19	1.14
7	Dizi (Wet-land)	SRI	0786623	0927792	1547	2.3.2022	23.7	6.77	355	11.5	3.0	7.4	12.0	2.33	75	2.20	1.48	0.64
8	Metu Mechi	SRI	0791930	0924109	1734	4.2.2022	18.5	7.81	295	12.59	2.78	4.76	6.75	0.68	70	2.40	0.35	-0.49
9	Shemane (Metu)	GWS	0789745	0920922	1669	26.2.2022	21.3	6.31	130	10.5	1.2	3.4	5.0	7.68	38	0.85	0.49	-1.96
10	Wobo (Yayu-Metu)	GWS	0809328	0923353	1550	1.3.2022	23.5	6.33	720	28.8	6.4	10.9	9.4	11.36	145	0.88	0.52	1.13
11	Wabo (Yayu-Elmo)	GWS	0808247	0924237	1561	1.3.2022	21.6	6.05	485	20.6	2.9	13.5	2.9	27.42	80	1.97	1.41	0.67
12	Becho (Sp)	GWS	0795311	0907730	1752	23.2.2022	25.0	5.65	143	15.6	1.4	5.5	13.1	8.41	77	1.06	0.38	0.47
13	Suphe	GWS	0793672	0942664	1654	2.3.2022	23.3	6.74	680	24.2	6.1	11.9	5.5	5.76	132	0.68	0.53	1.25
14	Nopha	GWS	0787763	0930935	1701	2.3.2022	22.2	5.87	1050	21.5	6.2	15.7	15.3	70.14	52	19.1	1.24	0.98
15	Ehud Gebeya	GWS	0785289	0911739	1683	28.2.2022	23.5	5.75	265	18.5	2.4	7.3	10.0	8.91	90	2.13	0.50	-0.55
16	Yember nr Chora	GWS	0839058	0924097	1890	24.2.2022	21.0	5.50	385	18.9	3.2	6.5	1.8	15.28	65	4.75	0.75	1.26
17	Dawe nr Achibo	GWS	0830706	0927100	1576	24.2.2022	21.5	6.50	1510	38.6	12.4	49.1	16.4	3.86	320	1.35	1.76	0.36
18	Bechano	GWD	0782480	0906560	1739	28.2.2022	23.9	5.80	215	16.1	1.3	6.4	3.4	10.77	60	1.70	0.48	1.58
19	Metu nr University	GWD	0781956	0920603	1654	26.2.2022	21.0	5.72	475	14.8	1.7	6.0	3.4	14.94	52	2.39	0.60	0.85
20	Ehud Gebeya Mosque	GWD	0785655	0911900	1738	28.2.2022	21.3	6.51	1190	21.6	4.2	11.0	59.6	20.56	35	11.6	33.43	0.09

Table 2 (continued)

S. no.	Location name	Source (origin)	Lon X (E) (UTM)	Lat Y (N) (UTM)	Elevation (m.a.s.l.)	Date collected	Temp. (°C)	pH	EC (µS/cm)	Cations (mg/L)			Anions (mg/L)			Ion balance error (%)		
										Ca <sup>2+</sup>	Mg <sup>2+</sup>	Na <sup>+</sup> K <sup>+</sup>	NO <sub>3</sub> -N	HCO <sub>3</sub> <sup>-</sup>	Cl <sup>-</sup>		SO <sub>4</sub> <sup>2-</sup>	
21	Gore Gumero Hotel	GWD	0779707	0902211	2003	28.2.2022	21.5	5.12	1060	20.5	3.4	17.0	13.0	1.26	72	4.62	15.50	0.50
22	Chora inside Hospital	GWD	0841808	0927057	1990	24.2.2022	21.6	5.00	110	10.8	0.8	4.2	7.5	13.22	35	1.37	2.15	0.53
23	Abono nr Chora	GWD	0835534	0925790	1633	23.2.2022	20.5	5.60	940	37.9	8.8	13.1	4.5	53.73	142	3.52	1.58	- 1.38
24	Geyi (Shoaber)	GWD	0787734	0921012	1633	4.3.2022	20.9	6.70	155	5.8	0.9	2.2	4.2	22	3.57	1.67	- 0.54	
25	Hurumu town	GWB	0795938	0922714	1783	4.3.2022	20.6	7.28	1556	47.0	18.1	20.3	10.0	5.47	290	0.89	0.88	0.50
26	Becho (DW)	GWB	0795447	0907094	1690	23.2.2022	25.0	6.45	1480	30.5	11.2	37.1	45.2	6.21	300	0.80	0.49	1.39
						Max	25.0	7.81	1556	46.97	18.14	49.1	59.6	70.14	320	19.1	33.4	1.58
						Min	18.5	4.80	110	5.77	0.76	2.18	1.77	0.68	12	0.68	0.35	- 1.96
						Avg	22.0	6.28	602.7	20.4	4.56	11.3	11.9	17.10	98.7	3.12	2.93	0.40

values against ‰ VSMOW. The two in-house solutions standardized using the IAEA's VSMOW2, SLAP2, and Greenland Summit Precipitation (GRES P) reference solutions were used for a two-point calibration. The 1st-reproducibility of an in-house water standard is δD: ± 1.2‰ and δ<sup>18</sup>O: ± 0.15‰ (n = 72); time-period covered: May 2021 to October 2022.

**Lineaments extraction**

The digital elevation model (DEM) was collected from the advanced land observing satellite-digital surface model (ALOS-DSM), accessed on 12 September 2019, and the GIS attribute maps were collected from the MoWE-Water Resources Information and GIS Desk. The existing geological map lacks sufficient structural information on the watershed lineaments. Automatic lineament extraction using PCI Geomatics was performed to fill the gap and aid the current map. Lineaments of the watershed were extracted from Landsat, the phased array L-band synthetic aperture radar (ALOS-PALSAR), after the application of image enhancement techniques as well as band filtering using PCI Geomatics 2020. Some of the processes applied were selecting the proper Landsat band, optimal parameterization, cleaning the extracted lines, and representing the line directions. Lineaments were identified by structural analysis and used to examine the groundwater movement and its interaction with surface water storage.

**Results and discussion**

**Hydrochemistry results**

Most cold groundwater is meteoric, i.e., composed of precipitated atmospheric moisture that has percolated through the zone of aeration (Linsley and Franzini 1979; Ward and Robinson 2000; Azagegn 2014). The water samples from the study area were meteoric and fresh. Evaluating the composition of these samples using laboratory analysis resulted in five water types of low mineralization; EC ranges from 97 for the rain to 3460 for deep wells and generally acidic to alkaline water with pH (4.02–9.46). The stream water, some springs, and water from shallow wells were predominantly Ca–HCO<sub>3</sub> type of recent recharge.

Chemical constituents present in groundwater are indicators of the rock minerals (Nonner 2003; Haile 2005; Clark 2015), and anthropogenic activities affect groundwater chemistry. Water type of Ca–NO<sub>3</sub> (Fig. 3) was found in shallow wells and springs near urbanized areas (Qidame Gebeya, Nopha, Tullube, and Metu University; S. No. 11, 13, 18, 20, respectively in Table 1) and Na–NO<sub>3</sub> in shallow wells

**Table 3** Results of the analysis of water samples for the Bega (secondary data)

S. no.	Location name	Source (origin)	Lon X (E) (UTM)	Lat Y (N) (UTM)	Elevation (m.a.s.l.)	Date collected	Temp. (°C)	pH	EC (µS/cm)	Cations (mg/L)				Anions (mg/L)			Ion balance Error (%)
										Na <sup>+</sup>	K <sup>+</sup>	Ca <sup>2+</sup>	Mg <sup>2+</sup>	Cl <sup>-</sup>	HCO <sub>3</sub> <sup>-</sup>	SO <sub>4</sub> <sup>2-</sup>	
<i>3. Data collected from Metu water resources office</i>																	
1	Yayu	GWB	0808423	0921873	1600	29.3.2016		7.26	563	33	3.8	73.6	25.9	5.33	424	0.31	1.61
2	Chora	GWB	0840586	0926380	1870	19.4.2009		6.98	327	43.5	2.8	27.7	6.63	4.12	220	1.6	1.82
3	Dizi	GWB	0786348	0926149	1650	19.3.2015		6.50	378	12.5	3	44	24	3.64	275	16.8	- 1.90
4	Ageta-kitabir	GWB	0791717	0931641	1775	5.7.2016	25	5.48	97	5.3	0.8	9.89	4.45	10.99	50	0	0.018
5	Metu Zuria	GWB	0786399	0918402	1540	Dec.2013		7.20	1580	222	23	129.6	25.4	18.2	1122	88.1	1.01
6	Sombo	GWD	0829587	0929783	1665	Dec.2013		7.81	365	22.5	8.2	57.6	11.5	5.46	268	1.71	4.31
7	Chora1	GWD	0840529	0918631	1916	Dec.2013		6.85	337	18	7.2	28.1	18.9	1	228	0.12	1.92
8	Chora2	GWD	0840610	0929700	1952	Dec.2013		7.70	318	19	6.3	37.8	10.2	1.03	215	0.19	- 0.13
9	Humbe	GWD	0840693	0940769	1964	Dec.2013		6.89	260	8.9	3.3	34.44	11.7	4.12	179	0.76	0.24
10	Chira	GWD	0840610	0929700	2008	Dec.2013		6.98	327	43.5	2.8	27.7	6.63	4.12	220	2	1.6
	SRI-Stream					<i>Max</i>		7.81	1580	222	23	129.6	25.90	18.20	1122	88.09	10.10
	GWS-Spring					<i>Min</i>		5.48	97	5.30	0.80	9.89	4.45	1.00	50	0.00	0.02
	GWD-Groundwater (Shallow, Dug)					<i>Avg</i>		6.97	455.2	42.82	6.12	47.04	14.54	5.80	320	13.70	2.04
	GWB-Groundwater (Borehole)																
	SPR-Precipitation																

located in Gore town inside the compound of Gumaro Hotel (S. No. 22). This type of water may be due to domestic waste disposal and pollution resulted from decayed organic matter.

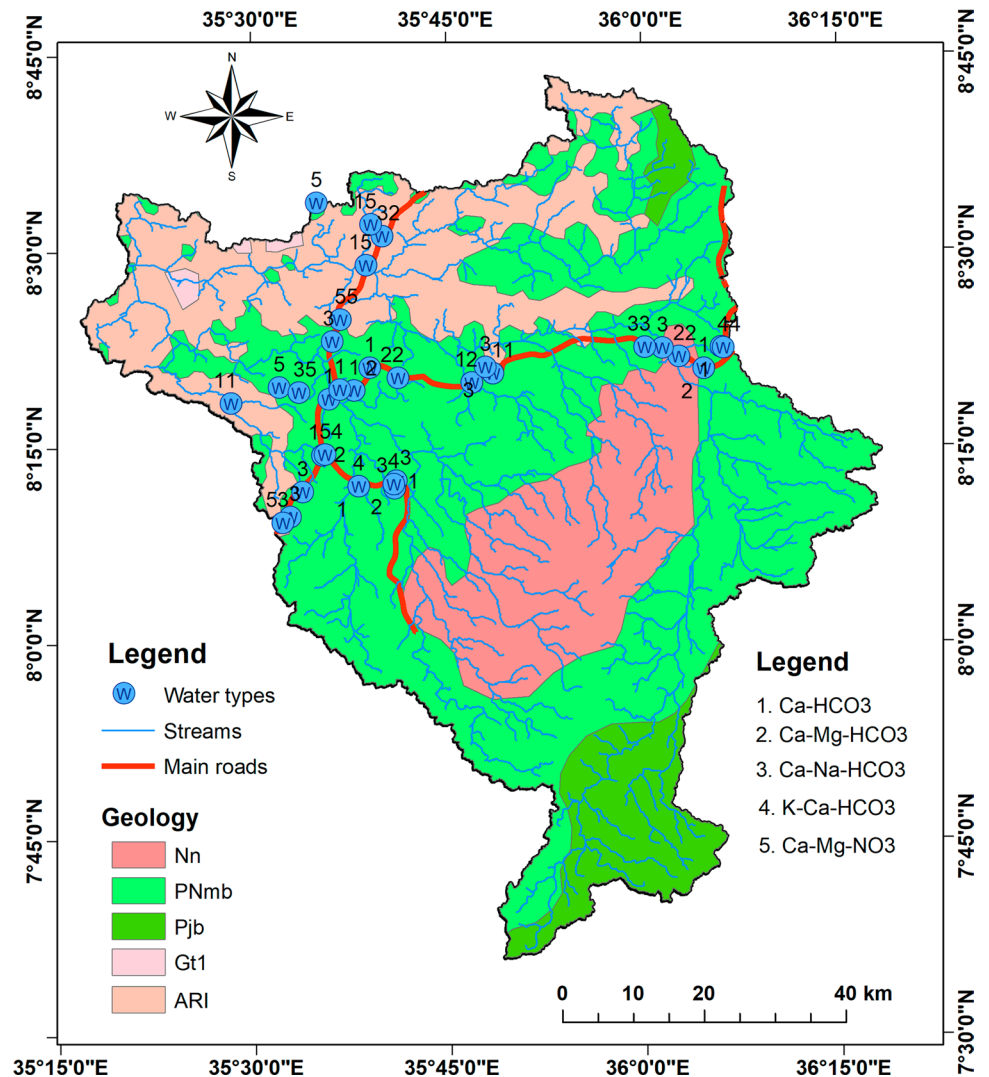
Groundwater quality in the watershed, especially in shallow wells and springs near settlements, is at risk because of anthropogenic pollution. High vulnerability where concentrations of  $\text{NO}_3^-$  exceeding the national and the WHO limit of 50 mg/L (ESA 2013; WHO 2017) reported within the watershed may be due to domestic waste pollution. Due to the shallow groundwater in the area,  $\text{NO}_3^-$  can quickly mix into the groundwater table. This is in line with Kebede (2013) and Zhang et al. (2021) showing that the presence of  $\text{NO}_3^-$  in groundwater indicates recent recharge and interactions between groundwater and surface water.  $\text{K}_2\text{-SO}_4$  type water was found at Ehud Gebeya near the mosque (S. No. 14 in Table 1). This open hand-dug well, used for cleansing purposes, is expected to be frequently contaminated by humans. Some of the water types are of  $\text{Ca-Mg-HCO}_3^-$  type, which may be due to the dissolution of volcanic rocks. The source

of  $\text{HCO}_3^-$  may be the dissolution of atmospheric and soil  $\text{CO}_2$ .

The observed low pH in groundwater (GWS, GWD, and GWB) is a signal of silicate weathering, dissolution of  $\text{CO}_2$  from the atmosphere, and the subsurface geologic formations that lead to the formation of  $\text{HCO}_3^-$ . The water type is related to natural processes like rock-water interaction and anthropogenic pollution like waste disposal. Some of the water types (Fig. 4) found on the Alge Group (ARI) and the Nazret Series (Nn) are of  $\text{Mg-HCO}_3^-$  and the Mekonnen basalts (PNmb) are of  $\text{Ca-HCO}_3^-$  types, whereas in shallow wells and springs around towns and settlements  $\text{Ca-NO}_3^-$  type showing a direct connection of groundwater and surface water.

The principal purpose of a Piper diagram is to show the grouping of samples and deduce the hydrochemistry or clusters of samples. The two triangles along the base give the relative compositions of cations (Na + K, Ca, and Mg) and anions ( $\text{Cl}$ ,  $\text{HCO}_3 + \text{CO}_3$ , and  $\text{SO}_4$ ) as a percentage of the

Fig. 3 Chemical water types of the study area



total cations or anions in meq/L. Total cations and anions are equal to 100%. Data points from the diamond grid are projections from the two triangles at the bottom. Most of the water samples shown in the left corner of the diamond grid were low-temperature, fresh, and calcium bicarbonate (Ca–Mg–HCO<sub>3</sub>) types. However, a few water samples above the bottom corner of the diamond grid show mixed intrusions for the Keremt 2020 and sodium chloride type for the Bega 2022 in the main water types. The water type refers to its hydrochemical or geochemical nature and the interaction between groundwater and surface water.

In general, the low ion concentrations (low mineralization) could be indicators of limited weathering and silicate dissolution. Relatively high concentrations of Ca<sup>2+</sup> and Na<sup>+</sup> from cations and HCO<sub>3</sub><sup>-</sup> from anion species are present in the watershed. The Pie chart (Fig. 5a) shows the mean parameter values of the applicable samples on a multiple-sample basis. The general dominance of anions was in the order HCO<sub>3</sub><sup>-</sup> >> Cl<sup>-</sup> > SO<sub>4</sub><sup>2-</sup> > NO<sub>3</sub><sup>-</sup>, and the predominance of cations was Ca<sup>2+</sup> > Mg<sup>2+</sup> > Na<sup>+</sup> > K<sup>+</sup>. Silicate weathering produces HCO<sub>3</sub><sup>-</sup>, but the dissolution of carbonate minerals is the primary source of Ca<sup>2+</sup> and Mg<sup>2+</sup> (Appelo and Postma 2005; Krishnaraj et al. 2012; Zhou et al. 2017). The Giggenschbach triangle (K–Mg–Na) representation, on the other hand, allows for verifying the extent that attains the rock-water equilibrium. The triangle comprises three parts: the immature bottom water, the center partly in equilibrium water, and the top curve entirely in equilibrium water. The waters found in all the samples from the watershed are immature (Fig. 5b).

Tables 1, 2, and 3 Show the variation in statistics of the analyzed water samples of the Keremt 2020, the Bega 2022, and other secondary sourced data.

The relation between hydrochemistry and the dominant natural processes (evaporation, rock-water interaction, and precipitation) can be analyzed using the Gibbs diagram (Gibbs 1970). The range of weighted ratio values of Na<sup>+</sup>/(Na<sup>+</sup> + Ca<sup>2+</sup>) is from 0.04 to 0.529, with an average of 0.297, whereas the Cl<sup>-</sup>/(Cl<sup>-</sup> + HCO<sub>3</sub><sup>-</sup>) ranges from 0.003 to 0.713 and an average of 0.109. As shown in Fig. 6, almost all the samples result for cations and anions are strongly controlled by the rock-water interaction dominance zone. This rock-water interaction ultimately manifests as the interaction between groundwater and surface water, as these sources are hydraulically linked in the region. Based on the summer (Keremt) 2020 anions and cations graph and winter (Bega) 2022 cations graph, the weighted ratio of Nopha spring, Gore Gumero Hotel shallow well, Dawe spring, and Becho deep well are observed to be far away from other points showing high mineralization, even though the dominant process is rock-water interaction.

### Isotope analysis results

Of all the methods used to understand hydrogeological processes in small watersheds, applications of tracers, particularly the isotopic signature of water, have been the most useful in providing new insights into hydrologic processes (Kendall and McDonnell 1998; Clark 2015). While working

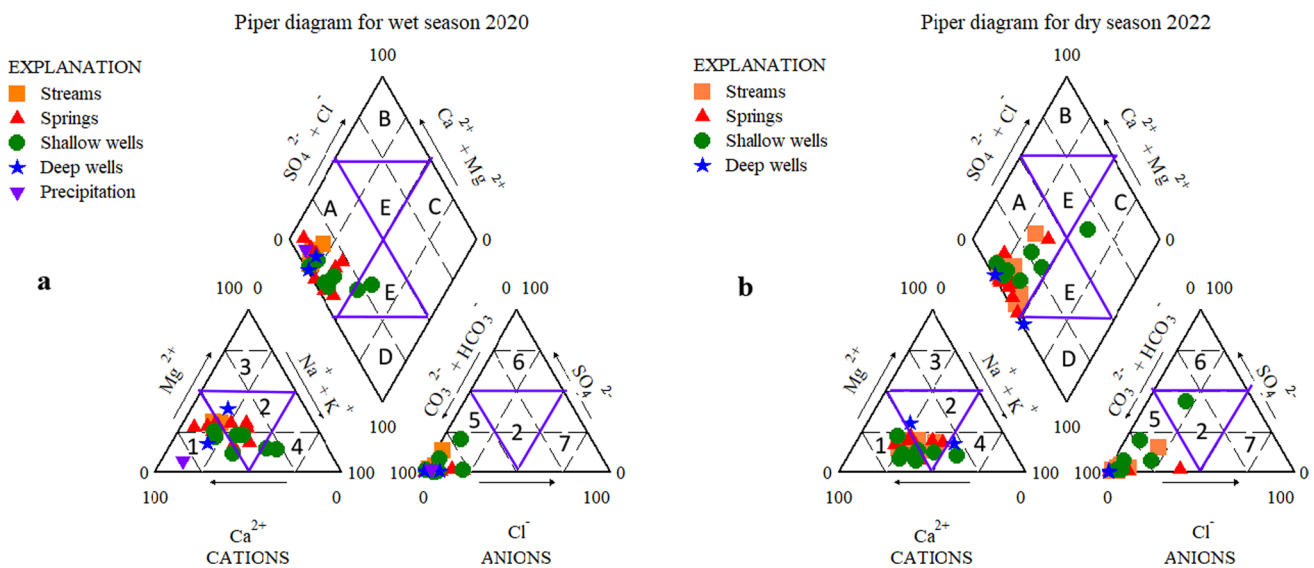


**Fig. 4** Piper diagram showing hydrochemical compositions and water types in the study area **a** Keremt 2020 **b** Bega 2022 (1) calcium type; (2) no dominant type; (3) magnesium type; (4) sodium type;

(5) bicarbonate type; (6) sulfate type; (7) chloride type; **A** Ca–HCO<sub>3</sub> type; **B** Ca–Cl type; **C** Na–Cl type; **D** Na–HCO<sub>3</sub> type; **E** mixed type



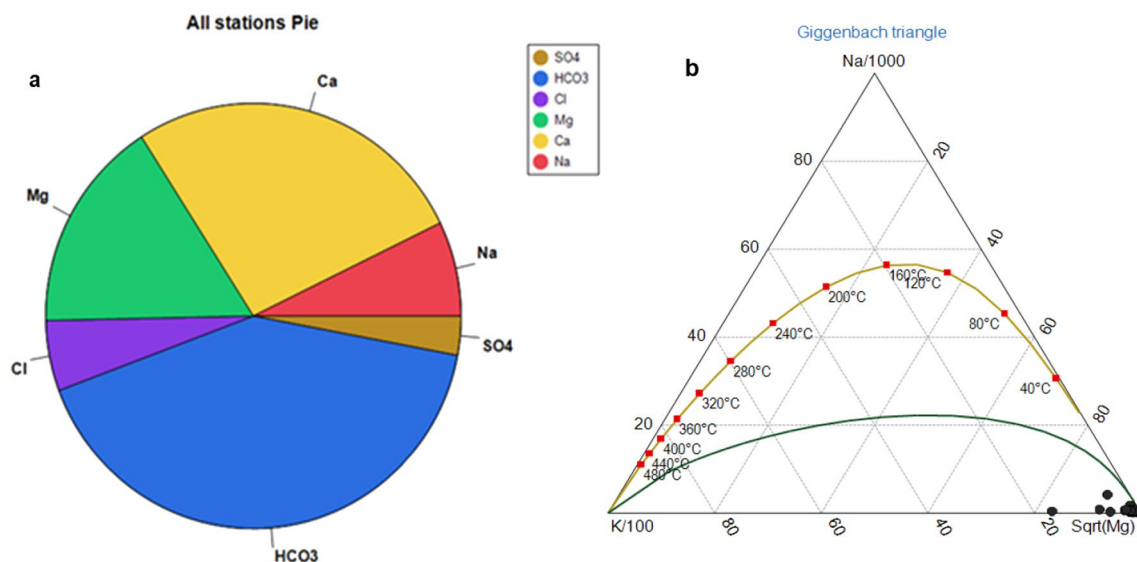


**Fig. 5** Mean distributions of major ions **a** pie chart and **b** Giggenbach triangle

on several samples taken from around the world, Harmon Craig (Craig 1961) found that the isotopic compositions of meteoric waters related to the linear regression equation of what is now the famous Global Meteoric Water Line (GMWL), written as (Eq. (4)):

$$\delta D = 8\delta^{18}O + 10 \quad (4)$$

where the values expressed per mille unit, intercept 10 is deuterium excess (d-excess) equals  $\delta D - 8\delta^{18}O$ , and the slope eight is the ratio of fractionation factor ( $\alpha D/\alpha^{18}O$ ). The plot of GMWL was based on average global values of  $\delta^{18}O$  and  $\delta D$ , meaning that specific regions or watersheds have their own Local Meteoric Water Lines (LMWL). The mean compositions of  $\delta D$  and  $\delta^{18}O$  isotopes in summer 2020 water samples from all sources are 3.93 and  $-1.48$  per mille (Table 4). The summer (Keremt) isotopic relationship connecting  $\delta D$  and  $\delta^{18}O$  values for all water samples for which data on both isotopes are available and presented by the linear regression equation (Fig. 7a) as:

$$\delta D = 7.6\delta^{18}O + 15.2 \quad (5)$$

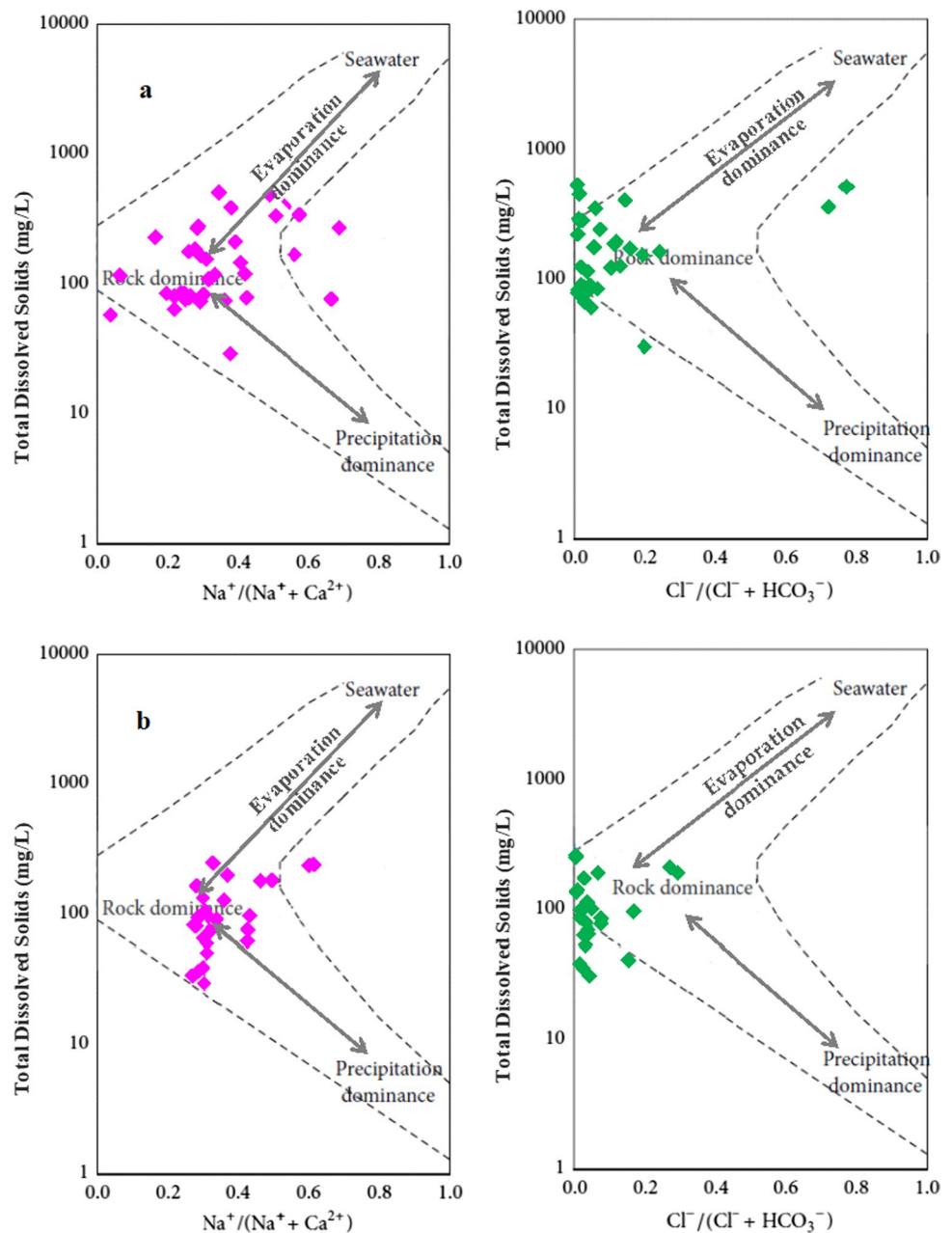
The equation shows an average slope of 7.6 and a d-excess of 15.2 (Eq. (5)). The higher d-excess may indicate the contribution from the water evaporated due to a dry climate with low relative humidity in the atmosphere (Fritz et al. 1979; Appelo and Postma 2005; Clark 2015). In the  $\delta D$  versus  $\delta^{18}O$  plot, the monthly rains of Addis Ababa express a local meteoric water line (AA-LMWL) defined by  $\delta D = 7.2\delta^{18}O + 11.9$  (Kebede and Travi 2012; Kebede et al. 2021), (Fig. 7b). A comparable plot of rains in summer at Addis Ababa has the linear relation:  $\delta D = 7.6\delta^{18}O + 13$ , and

that of the rains in spring is  $\delta D = 6.05\delta^{18}O + 13.7$  (Kebede and Travi 2012). Intense seawater evaporation in conditions of moisture deficit causes higher values of d-excess. Precipitation from waters with low sea surface temperature and higher relative humidity typically shows moderate to low d-excess (Vreča and Kern 2020).

The mean isotopic composition of  $\delta D$  and  $\delta^{18}O$  in winter meteoric water samples is 5.08 and  $-1.09$  per mille, and  $\delta D = 6.29\delta^{18}O + 11.91$  (Table 4). Deuterium and Oxygen-18 of the analyzed water samples plotted within the boundaries of meteoric water lines show that the representative samples' origins are meteoric. Most groundwater, stream water, and rainwater samples lay closer to the AA-LMWL, suggesting meteoric origin except for deviation to the left because of distance and altitude effects. The unique characteristics of waters in the watershed are the relatively excessive amount of D and  $^{18}O$  in it. There is a strong correlation between springs, shallow wells, and streams indicating the presence of GW–SW interaction and local recharge. Evidence for the effect of evaporation can be seen in Fig. 7b on the top right side for stream and marsh waters shown in an enclosure with  $\delta^2H$  average of 9.91 and a  $\delta^{18}O$  average of  $-0.32$ . Deep wells, some shallow wells, and springs show lower amounts of deuterium and Oxygen-18 that high altitude origins can explain.

As shown in Fig. 7a, values of  $\delta D$  versus  $\delta^{18}O$  of rainwater samples are at the top, deep wells and some shallow wells samples are at the bottom, indicating infiltrated groundwater, and springs, streams, and other shallow wells mixed in the middle. Figure 7b shows the values of  $\delta D$  versus  $\delta^{18}O$  of deep wells, some springs and shallow wells samples at the bottom representing infiltrated groundwater, shallow wells and most springs in the middle, and a mix of springs,

**Fig. 6** Gibbs diagrams showing the dominant phenomenon on water samples **a** summer 2020 and **b** winter 2022



streams, and marshes at the top. The position of all  $\delta D$  versus  $\delta^{18}O$  values lies on the left side of the LMWL. Mixing of  $\delta D$  versus  $\delta^{18}O$  values for most different water samples suggests the interaction of the various water sources.

In cases where the measured values shift from LMWL, the type of shifting provides information regarding the process (e.g., rock-water interaction, evaporation, and precipitation) leading to the observed shift. Evidence from hydrochemical ions data analysis indicates that the local groundwater flow system in the watershed is associated with rock-water interaction.

The NW–SE cross-section from the lowest to the highest elevation in the watershed, generated based on the

geological map (Fig. 2), enables the development of the local, intermediate, and regional groundwater flow system (Fig. 8). The groundwater flow system is gravity-driven and is a fundamental process in playing its role as a geologic medium (Toth 2009; Anderson et al. 2015; Woessner 2020). The local flow system partly drains to the springs and the streams and partly percolates and joins the groundwater system. Groundwater flows and finally finds its way back to the surface water bodies. As shown in Fig. 8, the flow system interconnects the different water sources, surface water, groundwater, and other sources, confirming the groundwater-surface water interaction.

**Table 4** Results of isotopic laboratory analysis for summer (Kerent) 2020 and winter (Bega) 2022

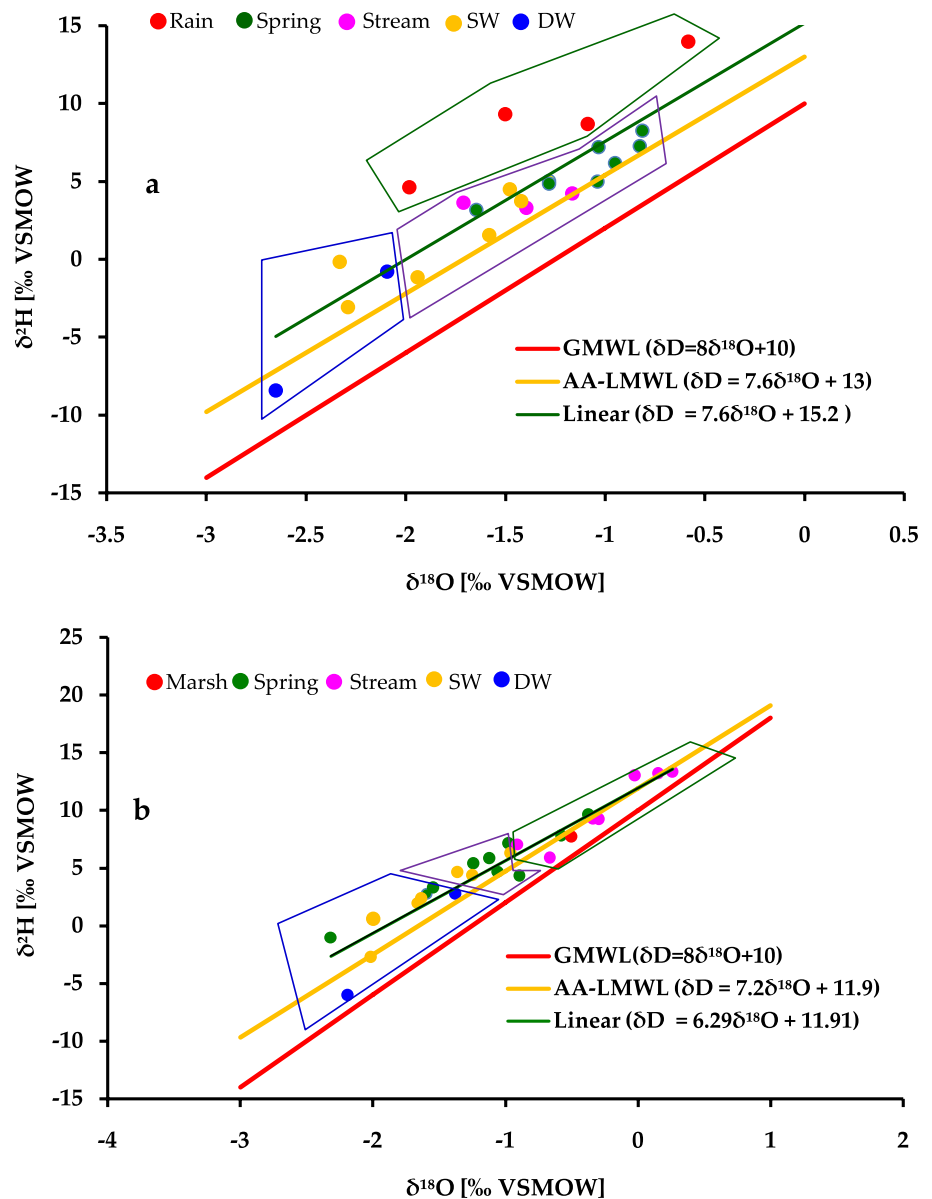
S. no.	Location name	Zone	Lon X (E) (UTM)	Lat Y (N) (UTM)	Elevation (m.a.s.l.)	Abbr	(% $\infty$ VSMOW) 2020		(% $\infty$ VSMOW) 2022	
							$\delta^2\text{H}$	$\delta^{18}\text{O}$	$\delta^2\text{H}$	$\delta^{18}\text{O}$
1	Metu Town	36P	0784327	0918296	1711	SPR	8.68	- 1.09		
2	Becho Town	36P	0795666	0908167	1781	SPR	4.60	- 1.98		
3	Nopha Town	36P	0787763	0930935	1701	SPR	9.30	- 1.50		
4	Gore Town	36P	0779301	0901863	2034	SPR	13.96	- 0.58		
5	Shemane nr Metu	36P	0789745	0920922	1669	GWS	4.97	- 1.04	4.32	- 0.90
6	Wobo nr Yayu-Metu	36P	0809328	0923353	1550	GWS	6.17	- 0.95	7.11	- 0.98
7	Wabo nr Yayu-Elemo	36P	0808247	0924237	1561	GWS	7.19	- 1.03	5.84	- 1.12
8	Becho nr High School	36P	0795311	0907730	1752	GWS	4.84	- 1.28	5.38	- 1.24
9	Qidame Gebeya	36P	0784391	0947363	1712	GWS	7.24	- 0.82		
10	Suphe	36P	0793672	0942664	1654	GWS	8.22	- 0.81	7.78	- 0.58
11	Nopha	36P	0787763	0930935	1701	GWS	3.16	- 1.64	2.78	- 1.60
12	Yember nr Chora	37P	0839058	0924097	1890	GWS	4.46	- 1.48	3.30	- 1.55
13	Nopha	36P	0787763	0930935	1701	GWS			2.78	- 1.60
14	Ehud Gebeya	36P	0785289	0911739	1683	GWS			4.70	- 1.06
15	Dawe nr Achibo	37P	0830706	0927100	1576	GWS			- 1.02	- 2.32
16	Tullube	36P	0779128	0921347	1670	GWD	1.52	- 1.58		
17	Becho	36P	0795666	0908167	1781	GWD	4.99	- 1.28	2.74	- 1.38
18	Metu nr University	36P	0781956	0920603	1654	GWD	- 1.16	- 1.94	1.98	- 1.66
19	Ehud Gebeya Mosque	36P	0785655	0911900	1738	GWD	- 3.09	- 2.29	4.38	- 1.25
20	Gore Gumero Hotel	36P	0779707	0902211	2003	GWD	- 0.19	- 2.33	0.57	- 2.00
21	Abono nr Chora	37P	0835534	0925790	1633	GWD	3.73	- 1.42	4.64	- 1.36
22	Metu nr University	36P	0781956	0920603	1654	GWD			1.98	- 1.66
23	Chora inside Hospital	37P	0841808	0927057	1990	GWD			2.34	- 1.63
24	Gegi Bechano	36P	0782480	0906560	1739	GWD			6.26	- 0.96
25	Geyi (Shoa ber)	36P	0787734	0921012	1633	GWD			- 2.75	- 2.02
26	Sor nr Metu	36P	0786141	0919692	1519	SRI	3.61	- 1.71	13.32	0.26
27	Saki nr Yayu	36P	0806355	0922062	1308	SRI	3.29	- 1.39	5.89	- 0.67
28	Qonnor nr Burusa	36P	0772335	0919052	1571	SRI	4.21	- 1.16	9.63	- 0.37
29	Qeber nr Kemise	36P	0790393	0907402	1674	SRI			13.18	0.15
30	Elike nr Suphe	36P	0792056	0944371	1570	SRI			9.23	- 0.30
31	Gebba nr Suphe	36P	0791389	0938602	1136	SRI			9.27	- 0.34
32	Gebba nr Chora	37P	0833214	0926994	1540	SRI			13.01	- 0.02
33	Dizi	36P	0786623	0927792	1547	SRI*			7.06	- 0.91
34	Metu Mechi	36P	0791930	0924109	1734	SRI*			7.69	- 0.50
35	Hurumu Town	36P	0795938	0922714	1783	GWB	- 8.45	- 2.65	- 6.03	- 2.19
36	Chora nr the Hospital	37P	0841515	0927141	1962	GWB	- 0.81	- 2.09		
	SRI-Stream or marsh					Max	13.96	- 0.58	13.32	0.26
	GWS-Spring					Min	- 8.45	- 2.65	- 6.03	- 2.32
	GWD-Groundwater (Shallow, Dug)					Avg	3.93	- 1.48	5.08	- 1.09
	GWB-Groundwater (Borehole)SPR-Precipitation									

## Conclusions

Investigating exchange fluxes has become essential in many research studies on groundwater and surface water interactions. This study applied a combination of major hydrochemical ions and environmentally stable isotopes

of precipitation, surface water, and groundwater to characterize the nature of GW–SW in the Sor and Gebba watershed. The data used are primary hydrochemical data (water samples collected from the field) and hydrochemical data collected for water supply (secondary data used for water quality analysis). The in-situ measured pH values varied

**Fig. 7**  $\delta D$  and  $\delta^{18}O$  relation with LMWL for samples **a** Keremt 2020 and **b** Bega 2022, SW = shallow well, DW = deep well



between 4.02 and 9.46, while the EC ranged from 97 to 3460  $\mu S/cm$ . These measurements indicate that the water samples exhibited acidity to moderate alkalinity regarding pH and weak to strong mineralization as to EC.

The analysis via Piper diagram shows that relatively fresh natural meteoric water of Ca–Mg–HCO<sub>3</sub> type has existed in many sampling locations of the watershed, despite anthropogenic pollution in water source locations near towns and settlements. The diagram also showed that most water samples are low-temperature (average 23 °C), fresh, and calcium bicarbonate (Ca–HCO<sub>3</sub>) types. However, a few water samples show mixed intrusions on the main water types, Ca–NO<sub>3</sub> and K<sub>2</sub>–SO<sub>4</sub>. The Gibbs diagram further indicates that the dominant natural process is rock-water interaction.

The mean isotopic composition ( $\delta D$  and  $\delta^{18}O$ ) of all meteoric summer (Keremt) water samples in the study area is 3.93 and – 1.48 per mille (with  $\delta D = 7.6\delta^{18}O + 15.2$  linear equation) and the mean isotopic composition ( $\delta D$  and  $\delta^{18}O$ ) of winter water samples is 5.08 and – 1.09 per mille represented with a linear equation of  $\delta D = 6.29\delta^{18}O + 11.91$ . These relationships have demonstrated the effect of evaporation in the watershed streams and marshes exposed to the atmosphere. Springs and shallow wells are in the middle, and deep wells are considered as a filtrate of recharge from high altitudes.

The main findings of this research are (a) the upland headwaters are recharge areas, and the Sor and Gebba stream valleys are discharge areas. The complexity and heterogeneity in geology resulted in various water types due

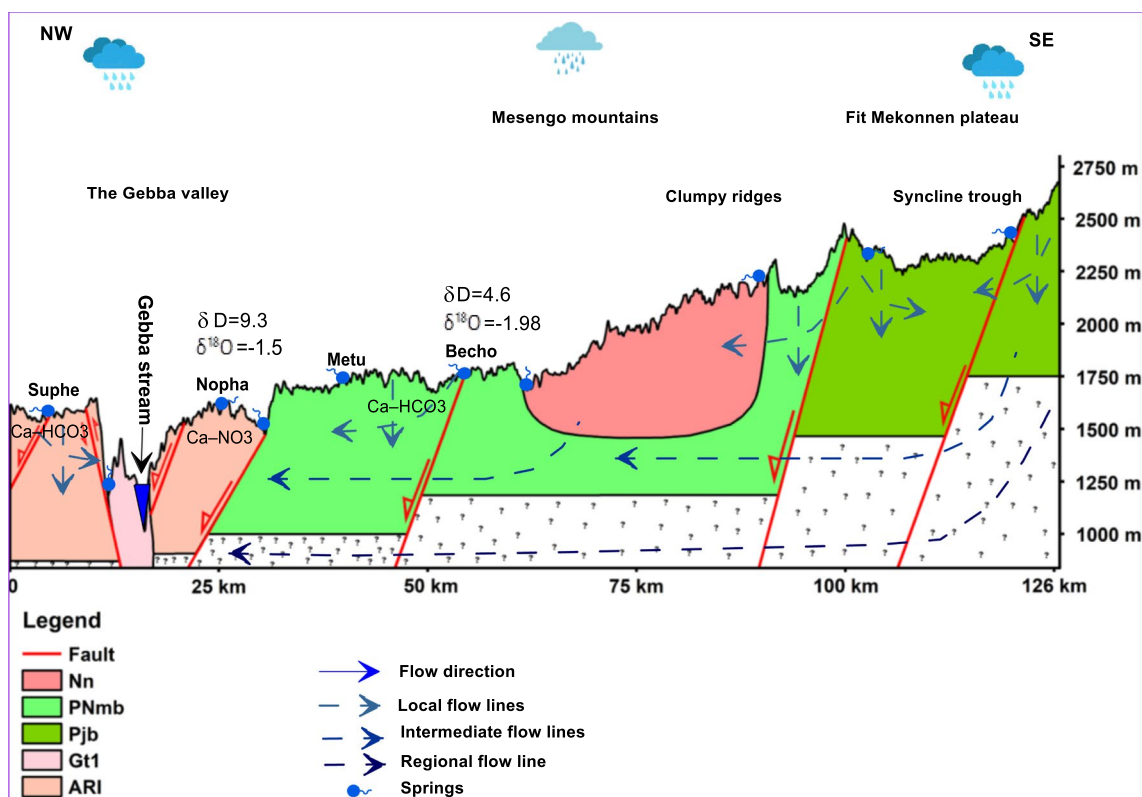


**Fig. 8** Schematic hydrogeological cross-section based on watershed geological map (Fig. 2) along the selected NW–SE line

to rock-water interaction, (b) hydrochemical results showed groundwater-surface water mixing in the watershed, and one can conclude that the flow direction is from groundwater storages to surface water bodies (streams and wetlands). The association of water types to natural and anthropogenic processes shows that if a specific water system is affected, it will quickly alter the other, and (c) depending on the isotopic analysis results, the water samples from all sources lay closer to the LMWL, supporting the hypothesis of meteoric origin. The correlation between the various water samples' isotopic ratios shows groundwater and surface water interaction in the watershed. This interaction indicates that most recharge is of recent meteoric water. These findings hold significant importance for the strategic planning, development, and management of the water resources in the Sor and Gebba watershed.

**Acknowledgements** The authors are grateful for the cooperation of many people and organizations in Germany and Ethiopia, in particular, Dr. Sylvia Riechelmann for isotope analysis and Mr. Nikolaus Richard and Mr. Oliver Schübbe for hydrochemical analysis at RUB, and Metu University for the logistic support. The authors would also like to thank the anonymous reviewers for their valuable comments and suggestions that helped to improve the manuscript.

**Author contributions** This article is part of the Ph.D. work of Wondmyibza Tsegaye Bayou, who performed material preparation, data

collection, and analysis and wrote the first draft of the manuscript. All authors contributed to the conception and design of the study, commented on earlier versions, and read and approved the final manuscript.

**Funding** Open Access funding enabled and organized by Projekt DEAL. We gratefully acknowledge the financial support from the German Academic Exchange Service (DAAD) sponsored by the EECBP Home Grown Ph.D. Scholarship Program, 2018 (Grant no. 57399471) for the first author. The funding also came from the Ministry of Education of the Government of Ethiopia. Thank you very much for the financial support.

**Data availability** The data presented in this study is available upon request from the corresponding author.

## Declarations

**Conflict of interest** The authors declare no conflicts of interest.

**Open Access** This article is licensed under a Creative Commons Attribution 4.0 International License, which permits use, sharing, adaptation, distribution and reproduction in any medium or format, as long as you give appropriate credit to the original author(s) and the source, provide a link to the Creative Commons licence, and indicate if changes were made. The images or other third party material in this article are included in the article's Creative Commons licence, unless indicated otherwise in a credit line to the material. If material is not included in the article's Creative Commons licence and your intended use is not permitted by statutory regulation or exceeds the permitted use, you will need to obtain permission directly from the copyright holder. To view a copy of this licence, visit <http://creativecommons.org/licenses/by/4.0/>.



## References

- Abid K, Dulinski M, Hadj Ammar F et al (2011) Deciphering interaction of regional aquifers. *Appl Geochem* 12
- Abteu W, Dessu SB (2019) The grand Ethiopian renaissance dam on the Blue Nile. In: Springer geography. Springer Geography, pp 1–11
- Alemayehu T (2006) Groundwater occurrence in Ethiopia. Addis Ababa University, Addis Ababa
- Alemayehu T, Kebede T, Liu L (2018) Basin characterization and determination of hydraulic connectivity of mega basins using integrated methods: (the case of Baro-Akobo and mega watershed beyond). *J Afr Earth Sci* 137:32–45. <https://doi.org/10.1016/j.jafrearsci.2017.09.011>
- Anderson MP, Woessner WW, Hunt RJ (2015) Applied Groundwater modeling: simulation of flow and advective transport, 2nd edn. Academic Press is an imprint of Elsevier
- Appelo CAJ, Postma D (2005) Geochemistry, groundwater and pollution, 2nd edn. A.A. Balkema Publishers, Leiden
- Azagegn T (2014) Groundwater dynamics in the left bank catchments of the Middle Blue Nile and the Upper Awash River Basins
- Barbieri M (2019) Isotopes in hydrology and hydrogeology. Water (Switzerland). <https://doi.org/10.3390/w11020291>
- Bayou WT, Wornlich S, Mohammed M, Ayenew T (2021) Application of hydrograph analysis techniques for estimating groundwater contribution in the sor and gebba streams of the baro-akobo river basin, southwestern Ethiopia. Water (Switzerland). <https://doi.org/10.3390/w13152006>
- Berhanu B, Seleshi Y, Melesse AM (2014) Surface water and groundwater resources of Ethiopia: potentials and challenges of water resources development. In: Nile River Basin: ecohydrological challenges, climate change and hydropolitics, pp 97–117
- Beyene S, Regassa A, Mishra BB, Haile M (2023) The soils of Ethiopia. Springer, Berlin
- Billi P (2015) Landscapes and landforms of Ethiopia
- Brooks KN, Ffolliott PF, Magner JA (2013) Hydrology and the management of watersheds, 4th edn. Wiley, Iowa
- Chernet T (1993) Hydrogeology of Ethiopia and water resources development 227
- Clark I (2015) Groundwater geochemistry and isotopes. Taylor and Francis Ltd, New York
- Clark I, Fritz P (1997) Environmental isotopes in hydrogeology. CRC Press, Boca Raton
- Craig H (1961) Isotopic variations in meteoric waters. *Am Assoc Adv Sci* 133:1702–1703
- Dawana YD (2020) Groundwater recharge estimation in Ethiopia. Dissertation, Addis Ababa University
- Devito KJ, Hill AR, Roulet N (1996) Groundwater-surface water interactions in headwater forested wetlands of the Canadian Shield. *J Hydrol* 181:127–147. [https://doi.org/10.1016/0022-1694\(95\)02912-5](https://doi.org/10.1016/0022-1694(95)02912-5)
- Dingman SL (2015) Physical hydrology, 3rd edn. Waveland Press, Inc., Long Grove
- ESA (2013) Ethiopian drinking water quality specifications. Ethiop Stand Agency 1–7
- Ezugwu CN, Apeh S (2017) Ground water and surface water as one resource: connectivity and interaction. *IOSR J Mech Civ Eng* 14:54–59. <https://doi.org/10.9790/1684-1403075459>
- FAO (1984) Geomorphology and soils. UNDP, FAO 804–804
- Fetter CW (2001) Applied hydrogeology, 4th edn. Prentice hall, New Jersey
- Freeze RA, Cherry JA (1979) Groundwater. Prentice-Hall. Inc., New Jersey
- Fritz P, Barker JF, Gale JE (1979) Geochemistry and isotope hydrology of groundwaters in the stripa granite
- Garrett AB (1962) The discovery of the oxygen isotopes. In: Giaque WF, Johnston HL. *J Chem Educ* 460
- Gibbs RJ (1970) Mechanisms controlling world water chemistry. *Am Assoc Adv Sci* 170:1088–1090
- Girmay E, Ayenew T, Kebede S et al (2015) Conceptual groundwater flow model of the Mekelle Paleozoic-Mesozoic sedimentary outlier and surroundings (northern Ethiopia) using environmental isotopes and dissolved ions. *Modèle conceptuel hydrogéologique d'écoulements des formations sédimentaires Paléoz. Hydrogeol J* 23:649–672. <https://doi.org/10.1007/s10040-015-1243-4>
- Graue WF, Johnston HL (1929) An isotope of oxygen, mass 18. *Nat Publ Gr* 123:34428
- Haile E (2005) Groundwater chemistry and recharge rate in crystalline rocks: case study from the Eritrean highland. Thesis, KTH Royal Institute of Technology
- Hunt RJ, Coplen TB, Haas NL et al (2005) Investigating surface water-well interaction using stable isotope ratios of water. *J Hydrol* 302:154–172. <https://doi.org/10.1016/j.jhydrol.2004.07.010>
- Kazmin V, Warden AJ (1975) Explanation of the geological map of Ethiopia. 212
- Kebede S (2013) Groundwater in Ethiopia features, numbers and opportunities. Springer Science+Business Media Dordrecht
- Kebede S, Charles K, Godfrey S et al (2021) Regional-scale interactions between groundwater and surface water under changing aridity: evidence from the River Awash Basin, Ethiopia. *Hydrol Sci J* 66:450–463. <https://doi.org/10.1080/02626667.2021.1874613>
- Kebede S, Travi Y (2012) Origin of the  $\delta^{18}\text{O}$  and  $\delta^2\text{H}$  composition of meteoric waters in Ethiopia. *Q Int* 257:4–12. <https://doi.org/10.1016/j.quaint.2011.09.032>
- Kebede S, Zewdu S (2019) Use of  $^{222}\text{Rn}$  and  $\delta^{18}\text{O}$ - $\delta^2\text{H}$  isotopes in detecting the origin of water and in quantifying groundwater inflow rates in an alarmingly growing lake, Ethiopia. Water (switzerland) 11:18. <https://doi.org/10.3390/w11122591>
- Kendall C, McDonnell JJ (1998) Isotope tracers in catchment hydrology, 3rd edn. Elsevier, New York
- King AC, Raiber M, Cox ME (2014) Analyse statistique multi variables de données hydro chimiques pour caractériser une connexion aquifère-cours d'eau alluvial durant sécheresse et hautes eaux: Cressbrook Creek, Sud-Est du Queensland, Australie. *Hydrogeol J* 22:481–500. <https://doi.org/10.1007/s10040-013-1057-1>
- Krishnaraj S, Murugesan V et al (2012) Use of hydrochemistry and stable isotopes as tools for groundwater evolution and contamination investigations. *J Geo-Sci* 1:16–25. <https://doi.org/10.5923/j.geo.20110101.02>
- Leontiadis IL, Nikolaou E (1999) Environmental isotopes in determining groundwater flow systems, northern part of Epirus, Greece. *Hydrogeol J* 7:219–226. <https://doi.org/10.1007/s100400050194>
- Linsley RK, Franzini JB (1979) Water resources engineering, 3rd edn. McGraw-Hill Book Company, New York
- Melesse AM (2011) Nile River Basin: hydrology, climate and water use. Springer Science+Business Media, Dordrecht
- Mengistu TD, Chung IM, Chang SW et al (2021) Challenges and prospects of advancing groundwater research in Ethiopian aquifers: a review. *Sustain* 13:15. <https://doi.org/10.3390/su132011500>
- Nonner JC (2003) Introduction to hydrogeology, 2nd edn. A.A. Balkema Publishers, Swets
- Ragheb M (2008) Isotope methods in water resources management 23
- Reimer A, Landmann G, Kempe S (2009) Lake Van, Eastern Anatolia, hydrochemistry and history. *Aquat Geochem* 15:195–222. <https://doi.org/10.1007/s10498-008-9049-9>
- Rundel PW, Ehleringer JR, Nagy KA (1989) Stable isotopes: history, units and instrumentation
- Stuyfzand PJ (1989) A new hydrochemical classification of water types. *IAHS Publ* 182:88–89
- Tarback EJ, Lutgens, Frederick K (2017) An introduction to physical geology, 12th edn. Pearson Education Limited, Harlow

- Tefera M, Chernet T, Haro W (1999) Explanation of the geological map of Ethiopia. Addis Ababa
- Terwey JL (1984) Isotopes in groundwater hydrology (Sudan). *Chall Afr Hydrol Water Resour Proc Harare Symp* 1984:155–160
- Toth J (2009) *Gravitational system of groundwater flow: theory, evaluation, utilization*. Cambridge University Press, New York
- Urey H (1931) A hydrogen isotope of mass 2. *J Chem Phys* 2872:164–165
- Vreča P, Kern Z (2020) Use of water isotopes in hydrological processes. MDPI AG, Switzerland This
- Wang J, Qin L, He H (2019) Assessing temporal and spatial inequality of water footprint based on socioeconomic and environmental factors in Jilin Province, China. *Water (switzerland)* 11:19. <https://doi.org/10.3390/w11030521>
- Ward RC, Robinson M (2000) *Principles of hydrology*, 4th edn. McGraw-Hill Publishing Company, Berkshire
- WHO (2017) *Guidelines for drinking-water quality*, 4th edn
- Woessner WW (2020) *Groundwater-surface water exchange*. Guellph, Ontario
- Yu X, Yuan X, Guo H et al (2022) Coupling hydrochemistry and stable isotopes ( $\delta^2\text{H}$ ,  $\delta^{18}\text{O}$  and  $87\text{Sr}/86\text{Sr}$ ) to identify the major factors affecting the hydrochemical process of groundwater and surface water in the lower reaches of the Yarlung-Zangbo River, Southern Tibet, Southwestern Chin. *Water (Switzerland)*. <https://doi.org/10.3390/w14233906>
- Zhang L, Li P, He X (2021) Interactions between surface water and groundwater in selected tributaries of the Wei River (China) revealed by hydrochemistry and stable isotopes. *Hum Ecol Risk Assess* 28:79–99. <https://doi.org/10.1080/10807039.2021.2016054>
- Zhou P, Li M, Lu Y (2017) Hydrochemistry and isotope hydrology for groundwater sustainability of the coastal multilayered aquifer system (Zhanjiang, China). *Geofluids*. <https://doi.org/10.1155/2017/7080346>

**Publisher's Note** Springer Nature remains neutral with regard to jurisdictional claims in published maps and institutional affiliations.